

# Structure of cooled Zn-Al eutectoid based alloys in biphasic domain

M. AGAPIE<sup>a\*</sup>, I. PETER<sup>b</sup>, B. VARGA<sup>a</sup>

<sup>a</sup>Transilvania University, Material Science Department, 29 Eroilor Blvd., 500036, Brasov, Romania

<sup>b</sup>Applied Science and Technology, Politecnico di Torino, Torino 10129, Italy

It is well-known that after solidification Zn-Al alloys, because of the high tendency of dendritic segregation, show a non-equilibrium structure with decomposition during the time. The eutectoid structure involves the presence of  $\beta$  phase, in the temperature interval of 275–430 °C. In the present research paper a systematically analyses concerning the structural modifications in the eutectoid Zn-Al alloys upon quenching at various heating temperatures has been considered and presented. The heat treatments applied to the alloy allowed the maintaining of  $\beta$  phase at room temperature. Dilatometric and differential calorimetric (DSC) analyses have allowed the evaluation of the stability of metastable  $\beta$  phase and revealed the structural changes that occur during heating. The microstructural analyses were performed by Optical microscopy.

(Received April 4, 2015; accepted October 25, 2015)

**Keywords:** Quenching, Microstructure, Dilatometric analysis, Differential calorimetric analysis, Zn-Al alloys, Phase transformation,  $\beta$  phase

## 1. Introduction

Zn-Al alloys with 5-30 wt% aluminium have a number of technological and exploitation properties that render them eligible for application in the most varied fields [1-6]. Outstanding technological properties, in particular their high fluidity, moderate melting and casting temperatures combined to energy-saving melting possibility make them an interesting solution also at industrial level. It is important to be mentioned that in the melting process of zinc at an overheating temperature of 100 °C, the energy consumption represents only 27 wt% of that required for melting aluminium at the same level of overheating.

As regards the exploitation properties one can remark their good corrosion strength, excellent cutting machinability and antifriction properties comparable to those of tin bronzes, actually considered as an ideal antifriction materials. The exploitation properties and their stability in time largely depend on the state of the structure at room temperature. The structural particularities at room temperature are determined by both the parameters of the crystallisation interval and the type of transformations in solid state as reported in Fig. 1.

It is well known that these transformations require long time that are, however, not guaranteed by the cooling rates encountered in the casting practice of parts and semi-finished products from these alloys. The structural non-homogeneity of hypereutectic compositions is determined by the shape of the liquidus and solidus curves. The shape of these curves determines a large distribution ratio ( $53/78= 0.68$ , for eutectoid compositions), contributing to the development of the structure outside equilibrium during the solidification process.

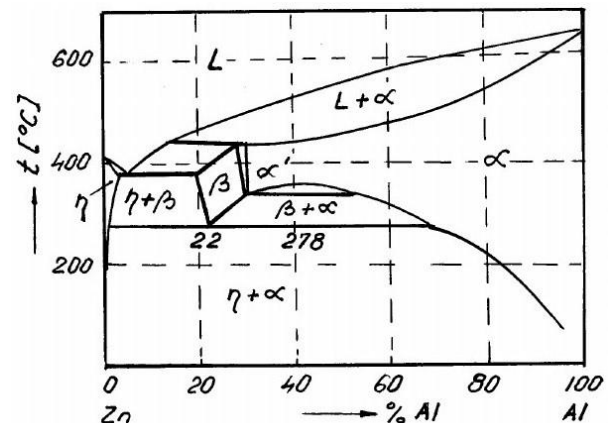


Fig. 1. Zn-Al thermal equilibrium diagram, after Presnyakov [3, 7].

During the phase transformation, at solidification, because of the high dendritic segregation, the eutectic can be present also in the compositions with 80 wt% aluminium [8, 9].

During exploitation the non-equilibrium structures characteristic for parts (semi-finished products) cast from these alloys tend to approach equilibrium structure thus determining the modification of the proportion of phases as well as of their nature.

The study of the structural transformations of Zn-Al alloys is interesting from an academic point of view, as they involve several types of transformations (solidification, peritectic reaction, eutectic and eutectoid decompositions) where the diffusion processes have a major role [10-13].

In this research paper a study of the phase transformations, in a eutectoid alloy as a function of the cooling mode, from both liquid and solid state, including from the two-phase area has been considered and presented.

## 2. Experimental determinations and results

Binary eutectoid alloy has been used for the experimental investigations.

The melting was realized in an electric graphite crucible with silit bars (electrical resistors), at a melting temperature of 700 °C and under a flux blanket.

The molten alloy was casted in metal moulds, in order to obtain ingots with a size of 14x160x80 mm size.

Fig. 2 reports the corresponding cooling curve, with indications of the temperatures of the inflection points corresponding to the phase transformations (the beginning and the end of crystallisation, the eutectic and the eutectoid transformations) and of the cooling rates in the intervals prior to the phase transformations.

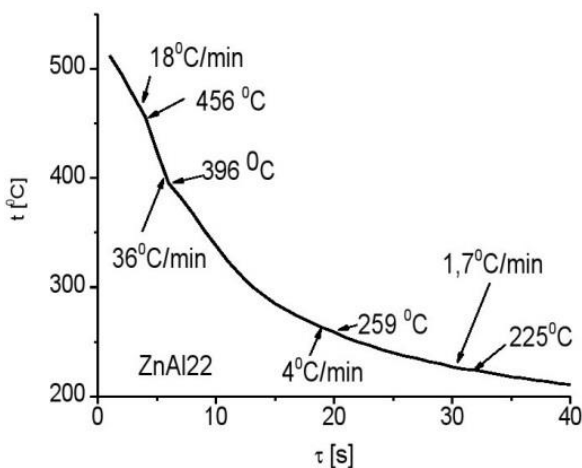


Fig. 2. Cooling curve for Zn-22 wt% Al alloy cast in metal moulds.

In Fig. 3 the structure of the cast alloy was reported.

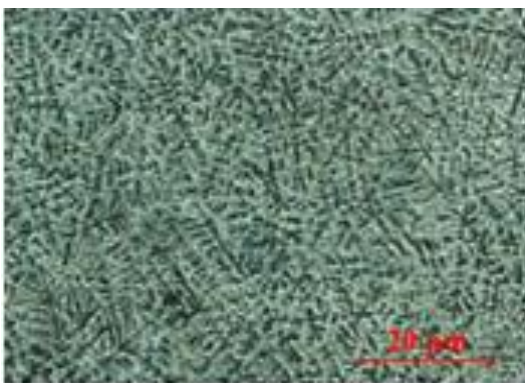


Fig. 3. Microstructure of the cast Zn-22 wt% Al alloy.

According to the thermal equilibrium diagram, at room temperature the structure should consist only of eutectoid phase. However, as can be noticed, it includes dendrites of  $\alpha$  solid solution characterised by a high dendritic segregation.

The inter-dendritic space consists of the eutectic developed at 382 °C.

Consequently, the structure obtained under the described cooling conditions differs significantly from the equilibrium one, because of the presence of both highly segregated  $\alpha$  solid solution dendrites and of the eutectic phase.

Based on the presented structure the amount of the eutectic phase in the structure of the alloy can be evaluated at 10%.

This value is in a good agreement with some literature data reported in [12, 13] obtained by theoretical calculation followed by experimental measurements.

By applying the inverse segments rule, considering that neither temperature nor the concentration of the eutectic point undergo modifications, a value of 24 wt% Al results for the maximum solubility point of zinc in  $\beta$  solid solution at eutectic temperature.

Considering this value, a so-called modified phase diagram can be plotted, as shown in Fig. 4.

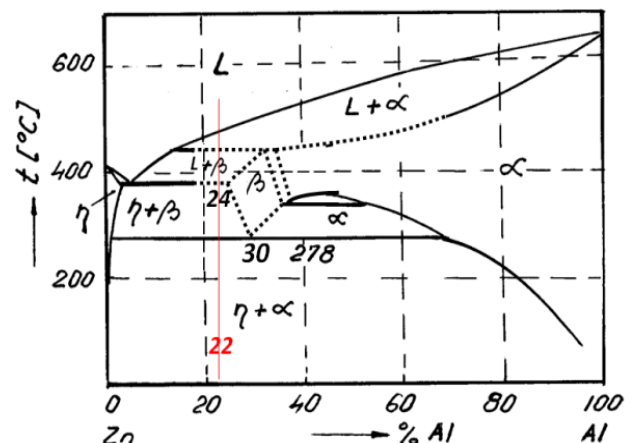


Fig. 4. Zn-Al modified phase diagram.

The modified diagram facilitates the interpretation of the real structures obtained at cooling rates recorded in the casting practice of parts from hypereutectic Zn-Al alloys. The modified phase diagram is in agreement with the proposed variants of diagrams [12, 13].

In order to obtain qualitative information on the crystallisation process, Fig. 5 reports the curves of the evolution of the solidified fraction ( $f_s$ ) in three conditions of solidification: the first one is according to the thermal equilibrium diagram (TED), the second one is related to the modified phase diagram (MPD) and finally the third one involves the controlled cooling.

For controlled cooling the variation curve of the solidified fraction was plotted by the DSC curve recorded at a cooling rate of 5 °C/min, as shown in Fig. 6.

The evaluation of the solidified fraction versus temperature considers both pro-eutectic and eutectic crystallisation phenomena (DSC).

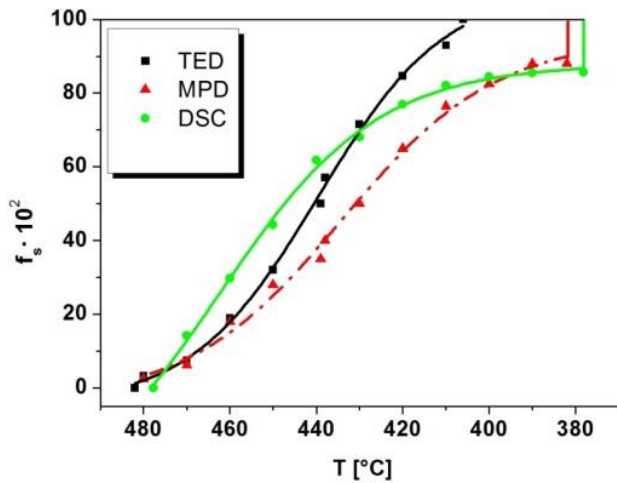


Fig. 5. Variation curves of the solidified fraction: according to the TED; according to the MPD and for DSC.

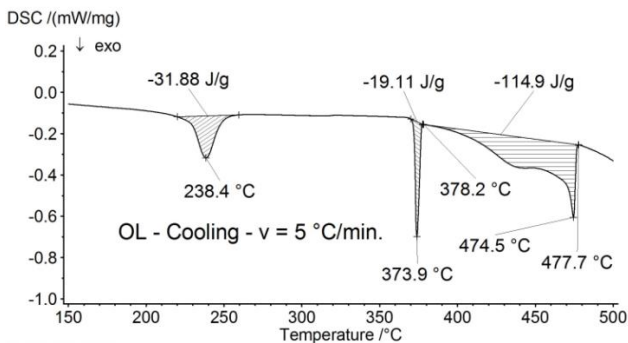


Fig. 6. DSC curve for Zn-22 wt% Al alloy cast in metal moulds.

It is important to underline that the eutectic transformation is present also in the cooling (solidification) of the alloy at a rate of 0.1 °C/min, as only a cooling rate of 0.06 °C/min ensures the solidification of the alloy at equilibrium, which is free of eutectoid transformation, as shown by the DSC curve reported in Fig. 7.

In order to generate a homogeneous equilibrium structure a two-step treatment was applied: solution hardening and maintaining of this solution at room temperature by rapid cooling (quenching) followed by annealing.

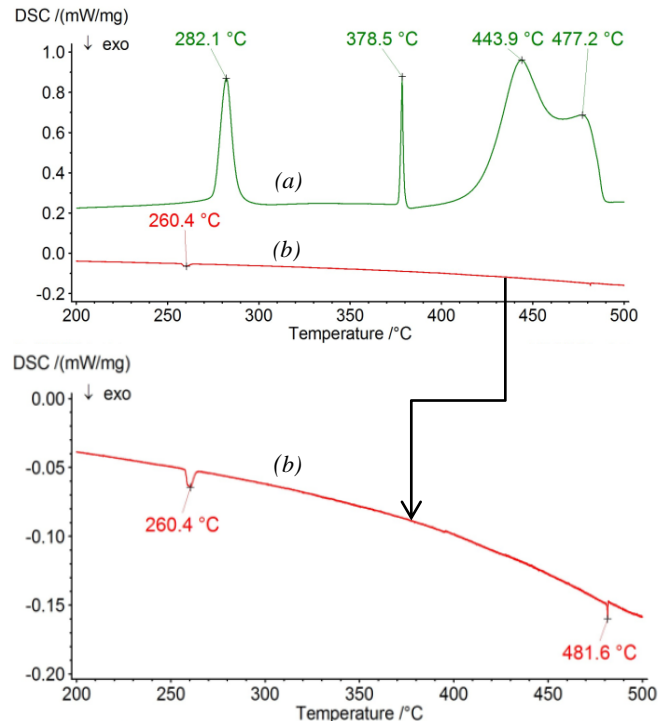


Fig. 7. DSC curve for Zn-22 wt% Al alloy at a: (a) heating (10 °C/min); (b) cooling rate of 0.06 °C/min

As in the case of the Zn-22 wt% Al alloy, solution hardening achieved by heating to 330-430 °C followed by actual quenching is aimed at maintaining  $\beta$  phase at room temperature, thus the development of a metastable structure. In the experimental determinations for the quenching of the heated alloy Jominy test was used.

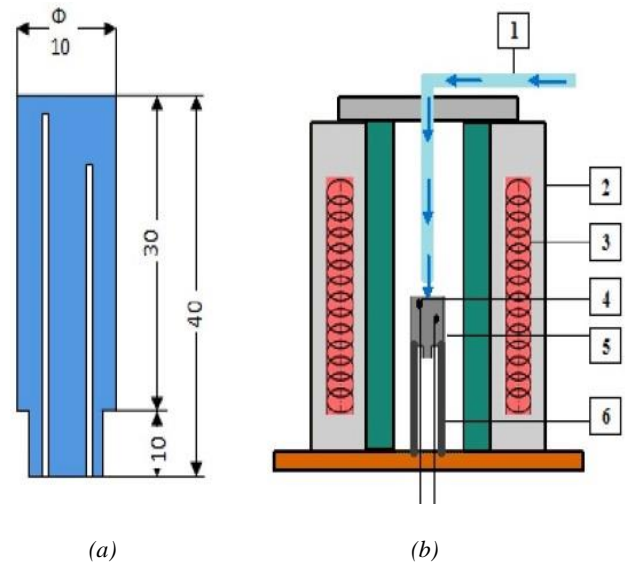


Fig. 8. Sketch of the quenching installation: a) Shape and dimensions of the samples; b) quenching device 1-water cooling system; 2-crucible; 3-electric resistance; 4-sample; 5-thermocouple; 6-sample support.

Considering the dimensions of the samples as shown in Fig. 8(a), a quenching device was conceived integrated into the crucible ensuring the heating, as illustrated in Fig. 8(b).

The thermocouples were placed into two pockets cut into the heat treated samples (Fig. 8(a)).

Fig. 9, reports the heating–maintaining–cooling curves for the three variants of heat treatments indicated by *I*, *II* and *III*.

In the case of heat treatments *I* and *II* temperature was recorded by means of two thermocouples. In the third heat treatment a single thermocouple was used, placed at the tip of the sample, as in treatments *I* and *II* no noticeable difference occurs between the two curves (Fig. 9).

The cooling temperatures recorded during the quenching of the sample are shown in the diagram of Fig. 9.

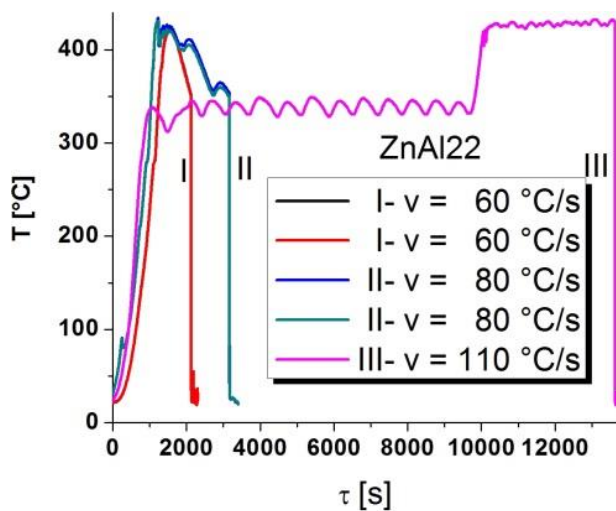


Fig. 9. Heating – maintaining – cooling curves for the three variants of heat treatments.

Fig. 10 reports the obtained microstructures for the 3 variants of heat treatments. Heat treatment variants *I* and *II* yielded a poly-phase structure, maintaining the solidification segregation of the dendrites.

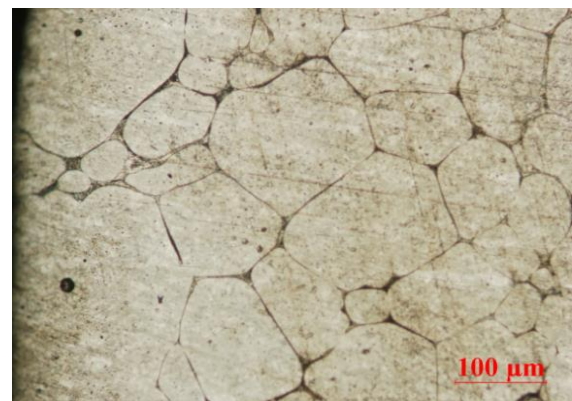
Fig. 10(a) shows the pocket cut for the thermocouple. The structure obtained consequently to the third variant of heat treatment consists of an approximately equiaxial  $\beta$  phase crystals.



(a)



(b)



(c)

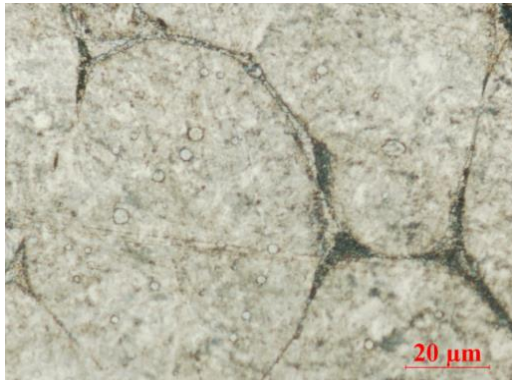
Fig. 10. Microstructure of the tips of the samples quenched by the three variants of heat treatment: (a) *I*; (b) *II*; (c) *III*.



The presence of very small amounts of eutectic (Fig. 10) has been observed at the limit of some crystals, Fig. 11. A stability analysis of  $\beta$  phase, metastable under certain conditions of heat treatment has complete, the present study.



(a)



(b)

Fig. 11. Microstructure showing the structure of the alloy quenched by treatment III: (a) granulation; (b) eutectic.

Thus, upon heating of the quenched sample to 400 °C, followed by 10 minutes maintenance and cooling at a rate of 5 °C/min, the metastable structure decomposed followed by the development of the phases (constituents) preannounced by the thermal equilibrium diagram and reported in the microstructure in Fig. 12. The particularity of the obtained structure consists in the fan-shaped arrangement of the eutectoid phases.

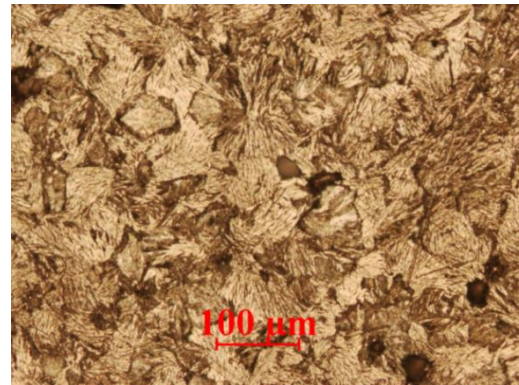


Fig. 12. Structure of the quenched sample upon annealing.

The structural study was completed by dilatometric and DSC analyses. Fig. 13 reports the primary dilatation-contraction curves (Delta-L-1 and Delta-L-2) for two heating-cooling procedures (Temperature 1 and Temperature 2, respectively). Heating at temperatures below the eutectoid one the total decomposition of the metastable  $\beta$  phase is insufficient. Additionally, to this observation, one can mention that at environmental temperature the metastable structure caused upon hardening (treatment III) remains stable even after 120 days, representing a novelty with respect to the results reported in the scientific literature data [14, 17] according to which the decomposition of  $\beta$  phase at room temperature occurs after approximately 10 days. One of the causes for this dissimilarity about the stability at room temperature of the metastable  $\beta$  phase has to be assigned to the specific modality of the heat treatment applied for the stabilisation of this phase involving different parameters.

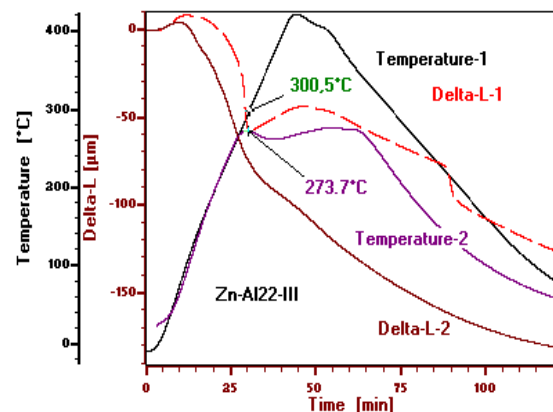


Fig. 13. Primary dilatation-contraction curves for the two heating-cooling procedures.

The dilatation-contraction and physical dilatation coefficient variation curves reported in Fig. 14 reveal the presence of inverse and direct eutectoid transformations at the heating of the quenched samples at over 400 °C.

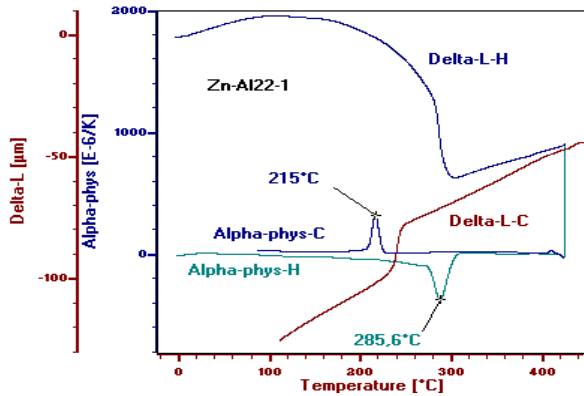


Fig. 14. The dilatation-contraction and physical dilatation coefficient variation curves for the "Temperature-1" procedure of Fig. 13 (H – heating, C – cooling).

The stability of the quenched structure is confirmed also by the DSC curves recorded for the cooling of the samples heated at temperatures above 279 °C and below 274 °C the eutectoid one (Fig. 15). In parallel the DSC curves for the heating (until melting) and cooling of the quenched samples (for all cases of heating/cooling the rate was of 10 °C/min) are reported.

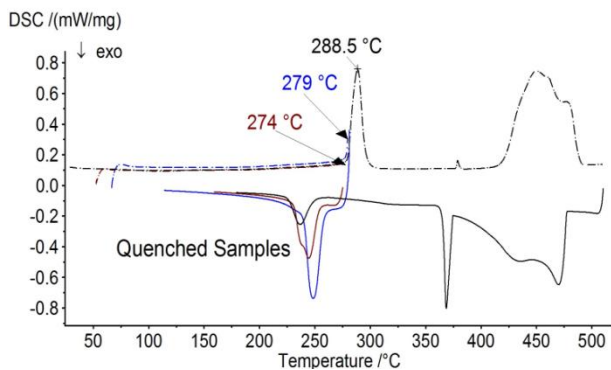


Fig. 15. DSC curves revealing the stability of phase  $\beta$  in the quenched alloy (— · — heating, — cooling).

It can be noticed that for the re-melting of the quenched samples, on the DSC curve after the melting of the residual eutectic, the melting within the entire volume progresses at higher temperatures according to the lines in the thermal equilibrium diagram, Fig. 16.

This phenomenon is attributed to the chemical homogeneity of the spherical  $\beta$  solid solution grains. In the case of cast structure alloys the peak for the inverse eutectic transformation is quite distinctive, and the melting of the alloy in its volume, because of the non-homogenous

composition of  $\alpha$  ( $\beta$ ) solid solution dendrites, progresses from this temperature.

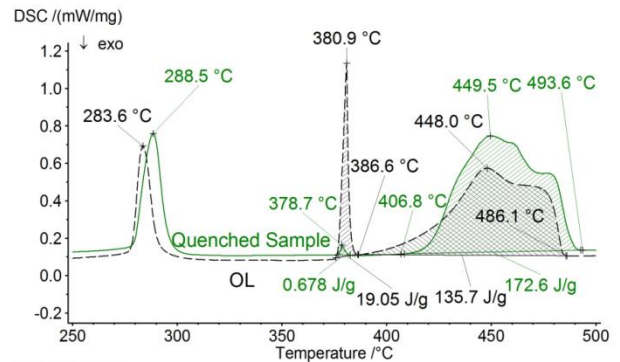


Fig. 16. DSC curves for the heating of alloys: a) cast structure alloys (---); b) quenched structure alloys (—).

The proportion of eutectic in these two structures can be estimated by calculating the surface areas (the latent melting heat values) corresponding to the phase transformations (eutectic  $\rightarrow$  liquid and  $\alpha$  solid solution  $\rightarrow$  liquid, and respectively eutectic  $\rightarrow$  liquid and  $\beta$  solid solution  $\rightarrow$  liquid) for the heating-melting of the two structures: in the metal moulds cast alloy the proportion of the eutectic corresponds to 12.3%, while in the quenched alloy it is 0.39%.

### 3. Conclusions

In this research paper the use of the modified phase diagrams was suggested to evaluate the solidification structures obtained in industrial metal moulds casting conditions.

Homogenisation of the casting structure and its quenching from the liquid – solid area guarantees the stability of the  $\beta$  phase at room temperature. The obtained metastable phase has long-term stability over 120 days. The total decomposition of metastable  $\beta$  phase is achieved only for heating above the eutectoid temperature.

The development of a finely structured and rosette shaped equilibrium phases (constituents) arises following the annealing of the metastable  $\beta$  phases.

A decrease of volume occurs following the decomposition of the metastable  $\beta$  phase.

### Acknowledgements

The authors wish to acknowledge the Structural Funds Project, Sectoral Operational Programme Human Resources Development (SOP HRD), ID137516 and the Structural Funds Project PRO-DD (POS-CCE, O.2.2.1., ID 123, SMIS 2637, ctr. No 11/2009) financed from the European Social Fund and by the Romanian Government respectively for providing the infrastructure used in this research work.

## References

- [1] M. A. Savas, S. Altintas, *J. Mater. Sci.* **28**, 1775 (1993).
- [2] Y. H. Zhu, *J. Mater. Sci.* **36**, 3973 (2001).
- [3] Y. H. Zhu, K. C. Chan, G. K. H. Pang, T. M. Yue, W. B. Lee, *J. Mater. Sci. Technol.* **23**, 347 (2007).
- [4] X. L. Xu, Z. W. Yu, S. J. Ji, J. C. Sun, Z. K. Hei, *Acta Metall. Sin.* **14**, 109 (2001).
- [5] G. Torres-Villaseñor, E. Martínez-Flores, in: J. Cuppoletti (Ed.), *Metal, Ceramic and Polymeric Composites for Various Uses*, Intech, Rijeka, Croatia (2011).
- [6] I. Peter, B. Varga, M. Rosso, *Mater. Sci. Forum* **790-791**, 223 (2014).
- [7] A. A. Presnyakov, Y. A. Gotban, V. C. Cherptyakova, *Russ. J. Phys. Chem.* **33**, 623 (1961).
- [8] A. Krupkowski, A. Pawlovski, B. Dukiet-Zawadzka, *Arch. Hutn.* **14**, 295 (1969).
- [9] R. Ciach, B. Dukiet-Zawadzka, T.D. Ciach, *J. Mater. Sci.* **13**, 2676 (1978).
- [10] Y.H. Zhu, *Mater. Trans.* **45**, 3083 (2004).
- [11] A. Sandoval-Jiménez, J. Negrete, G. Torres-Villasenor, *Mater. Charact.* **61**, 1286 (2010).
- [12] H. J. Dorantes-Rosales, V. M. Lopez-Hirata, J. Moreno-Palmerin, N. Cayetano-Castro, M. L. Saucedo-Muñoz, A. A. Torres Castillo, *Mater. Trans.* **48**, 2791 (2007).
- [13] H. J. Dorantes-Rosales, V. M. Lopez-Hirata, J. L. Mendez-Velazquez, M. L. Saucedo-Munoz, D. Hernandez-Silva, *J. Alloys Compd.* **313**, 154 (2000).
- [14] M. A. M. Arif, M. Z. Omar, N. Muhamad, J. Syarif, P. Kapranos, *J. Mater. Sci. Technol.* **29**, 765 (2013).
- [15] M. A. M. Arif, M. Z. Omar, N. Muhamad, *Pertanika J. Sci. & Technol.* **20**, 121 (2012).
- [16] T. J. Chen, Y. Hao, J. Sun, *Mater. Sci. Eng.* **337**, 73 (2002).
- [17] Z. M. Zhang, J. C. Wang, G. C. Yang, Y. H. Zhou, *J. Mater. Sci.* **35**, 3383 (2000).

---

\*Corresponding author: agapiemirela@yahoo.co.uk